Internal rotation, Stark effect, and rotational magnetic moments in CH_3CD_3

IRVING OZIER
Department of Physics, University of British Columbia, 6224 Agriculture Road, Vancouver, B.C., Canada V6T 2A6

AND

W. LEO MEERTS
Fysisch Laboratorium, Katholieke Universiteit, Toernooiveld, 6525 ED Nijmegen, The Netherlands

Received May 31, 1984

Ethane-1,1,1-d_3 has been studied by the electric-resonance molecular-beam method. By anticrossing techniques, the zero-field energy differences for $J = 1$ and 2 have been measured corresponding to the normally forbidden selection rules ($J \leftrightarrow J$), ($K = \pm 1 \leftrightarrow \mp 1$), and ($\sigma = \mp 1 \leftrightarrow 0, \mp 1$). From these splittings, three splitting ratio measurements, and four existing R-branch microwave frequencies, determinations were made of the moment of inertia of the CH_3-top $I_\alpha = 3.1549(12)$ amu Å^2 and of the effective height of the threefold barrier to internal rotation $V_3 = 1004.13(21)$ cm^{-1}, as well as of B and several distortion constants. From the current CH_3CD_3 value of V_3 together with previous values for asymmetrically deuterated forms of ethane, it has been shown that the change of V_3 with deuteration is $-3.05(13)$ cm^{-1} per deuteron. By conventional beam methods, the Stark and Zeeman effects have been studied. The Stark measurements have been analysed in terms of the anisotropy ($\alpha_\parallel - \alpha_\perp$) in the polarizability and the effective dipole moment for the matrix elements diagonal in J, namely $\mu_Q = \mu_0 + \mu_J J(J+1) + \mu_K K^2$. It has been found that $\mu_0 = 0.0108617(5)$ D, $\mu_J = 0.809(53)$ μD, $\mu_K = -2.06(10)$ μD, and $(\alpha_\parallel - \alpha_\perp) = 0.672(27) \times 10^{-24}$ cm^3. The two molecular g factors have been measured, $g_\parallel = 0.16451(25)$ nm and $g_\perp = 0.00325(16)$ nm, and the anisotropy ($\chi_\parallel - \chi_\perp$) in the magnetic susceptibility has been evaluated.

L'éthane-1,1,1-d_3 a été étudié par la méthode résonance électrique – faisceau moléculaire. Au moyen des techniques de croisement inverse, on a calculé les différences d'énergie à champ nul pour $J = 1$ et 2 correspondant aux règles de sélection normalement interdites ($J \leftrightarrow J$), ($K = \pm 1 \leftrightarrow \mp 1$) et ($\sigma = \mp 1 \leftrightarrow 0, \mp 1$). Les mesures de ces séparations, de trois rapports de séparation et de l'existence de quatre fréquences micro-onde dans la branche R ont permis la détermination du moment d'inertie de la toupie CH_3, $I_\alpha = 3{,}1549(12)$ uma Å^2 et de la hauteur effective de la barrière ternaire à la rotation interne, $V_3 = 1004{,}14(21)$ cm^{-1}, ainsi que de B et de plusieurs constantes de distorsion. De la valeur actuelle V_3 de CH_3CD_3, ainsi que des valeurs antérieures pour des formes deutérées asymétriques de l'éthane, on a montré que la variation de V_3 lors du marquage au deutérium est $-3{,}05(13)$ cm^{-1} par deutéron. Au moyen des méthodes conventionnelles de faisceau, les effets Stark et Zeeman ont été étudiés. Les mesures de l'effet Stark ont été analysées en terms de l'anisotropie ($\alpha_\parallel - \alpha_\perp$) de la polarisabilité et du moment dipolaire effectif pour les éléments de matrice diagonaux en J, à savoir $\mu_Q = \mu_0 + \mu_J J(J+1) + \mu_K K^2$. Il a été trouvé que: $\mu_0 = 0{,}0108617(5)$ D, $\mu_J = 0{,}809(53)$ μD, $\mu_K = -2{,}06(10)$ μD et $(\alpha_\parallel - \alpha_\perp) = 0.672(27) \times 10^{-24}$ cm^3. Les deux facteurs g moléculaires ont été mesurés, $g_\parallel = 0{,}16451(25)$ nm et $g_\perp = 0{,}00325(16)$ nm, et l'anisotropie ($\chi_\parallel - \chi_\perp$) de la susceptibilité magnétique a été évaluée.

[Traduit par le journal]

Can. J. Phys. **62**, 1844 (1984)

1. Introduction

Ethane is the simplest, most fundamental molecular system that undergoes internal rotation. However, because of the high degree of symmetry of the full protonated form of ethane, it has not been possible to date to carry out a detailed precision study of internal rotation in CH_3CH_3 itself. Not only is the permanent moment zero so that conventional microwave methods and the electric-resonance avoided-crossing technique (1, 2) are not available, but also the torsional transitions are strongly forbidden. The best direct measurement reported to date for the height V_3 of the hindering potential was determined (3) from the very weak torsional fundamental at about 289 cm^{-1}. Recent work (4–6) on the vibrational band ν_9 at high resolution may ultimately lead to a precision study of the second torsional overtone.

By partially deuterating CH_3CH_3, a small permanent dipole moment μ is introduced that allows the pure rotational spectrum to be studied. Hirota and coworkers (7–10) have observed the spectra of a variety of deuterated species. For the asymmetric tops (9, 10), accurate values of V_3 have been obtained within the framework of the standard models (11, 12) for internal rotation. From the variation of V_3 with deuteration, an extrapolation to the value for CH_3CH_3 was carried out.

From many points of view, CH_3CD_3 is the simplest of the many deuterated forms. Because it is a symmetric top, a full study of the internal rotation problem involves the fewest theoretical complications. Unfortunately, the conventional microwave spectrum for a symmetric rotor does not provide a direct measurement of V_3. The leading barrier-dependent terms in the energy depend only on quantum numbers that are

conserved in electric dipole transitions within the vibronic state. These terms therefore do not affect the pure rotational spectrum. No measurement of V_3 was possible from the microwave spectrum observed (7, 8).

With the development of the molecular-beam, electric-resonance avoided-crossing method (1, 2), it is now possible to make direct measurements in symmetric tops of the torsional splittings within a given torsional state and hence determine V_3. In this technique, two levels with Stark effects of opposite sign are brought to an avoided-crossing by applying a homogeneous electric field ϵ. The value of ϵ at which the difference Δ_0 in the zero field energies is cancelled by the difference Δ_s in the Stark energies is termed the crossing field ϵ_c. For $\epsilon \sim \epsilon_c$, it is effectively possible to violate the selection rules that require the conservation of the rotational quantum number K and the torsional quantum number $\sigma = -1, 0, +1$ that labels the torsional sublevels. *Rotational* anticrossings in which $\Delta J = 0$ but $\Delta K = \pm 1, \pm 2$, or ± 3 have been observed in CH_3CF_3 (1) and CH_3SiF_3 (13). These allow for a determination of A as well as for a study of the internal rotation problem. However, when $(A - B)$ is large as in CH_3SiH_3 or CH_3CD_3, the value of ϵ_c for these anticrossings its too high. One method of overcoming this difficulty is to study *barrier* anticrossings, as has been done in CH_3SiH_3 (14) and CH_3SiF_3 (13). In this case, $K = +1 \leftrightarrow -1$ so that $|K|$ does not change and the zero field separation Δ_0 is entirely due to the internal rotation (14).

The primary purpose of this current work has been to use the avoided-crossing method to observe barrier anticrossings in CH_3CD_3. Perhaps the most unusual feature of this experiment is the fact that it involves Stark tuning levels in a molecule whose dipole moment μ arises only from isotopic substitution: the magnitude of μ was known (7) to be only 0.01078(9) D. In spite of this, the value of ϵ_c was attainable because ϵ_c depends on Δ_0/μ and Δ_0 is small, being less than 30 MHz in the ground-torsion state. The results obtained for V_3 and several other internal rotation parameters are listed in Table I. With the present value of V_3 in CH_3CD_3, the extrapolation procedure used to obtain V_3 in CH_3CH_3 (10) has been tested and used to obtain an improved value. The current molecular-beam study of CH_3CD_3 also provided an important starting point for the analysis of the torsional spectrum ($\Delta v = +1$) that has now been observed[1] at considerably higher resolution than in the original report (3). A combination of the anticrossing and torsional data with those from the literature should further improve the present understanding of internal rotation in ethane.

[1]See M. Wong, H. Jagannath, and I. Ozier (manuscript in preparation).

TABLE I. Molecular constants for CH_3CD_3

Quantity	Units	Value
μ_0	D	0.0108617(5)[a]
μ_J	μD	0.809(53)
μ_K	μD	−2.06(10)
$(\alpha_\parallel - \alpha_\perp)$	10^{-24} cm^3	0.672(27)
$g_\parallel$	nm	+0.16451(25)[b]
$g_\perp$	nm	+0.00325(16)[b]
$(\chi_\parallel - \chi_\perp)$	10^{-30} J/T^2	−90.2(1.5)[c]
A	MHz	53 499(11)[d]
B	MHz	16 503.81(8)
D_J	kHz	19.5(1.4)
D_{JK}	kHz	49.3(6.6)
D_K	kHz	142.1[e]
ρ		0.3339792(22)
s		55.6277(18)
V_3	cm^{-1}	1004.13(21)[f]
F_{3J}	MHz	−143(9)
D_{Jm}	MHz	2.55(9)
d_J	MHz	6.18(27)
I_α	amu Å^2	3.1549(12)[g]

[a]The ratio of μ_0 to μ(OCS) is known slightly more accurately. With μ(OCS) = 0.71519 D from ref. 25, $\mu_0(CH_3CD_3)/\mu(OCS)$ = 0.01518713(45).

[b]Only the magnitudes and relative signs of the g factors were determined experimentally. The absolute sign was taken from comparisons with other molecules and susceptibility arguments. See Sect. 5.

[c]This was calculated using $\theta_\parallel = -2.67(33) \times 10^{-40}$ cm^2 from ref. 30. See Sect. 5.

[d]This was calculated from I_a = 9.4465(20) amu Å^2 as deduced from ref. 10 and ref. 36. See Sect. 7.

[e]This was held fixed. The value is taken from the force-field calculation of ref. 33. See Sect. 7.

[f]The least squares analyses assume $V_6 = 0$.

[g]This was calculated from ρ using I_a = 9.4465(20) amu Å^2 as deduced from ref. 10 and ref. 36. See Sect. 7.

The second purpose of the current work is to study the Stark and Zeeman effects. While both studies were essential to the analysis of the avoided-crossing data, each effect is interesting in its own right. It has been possible for the first time to determine the effects of centrifugal distortion on the parallel moment of CH_3CD_3 and to measure the anisotropy $(\alpha_\parallel - \alpha_\perp)$ in the static polarizability. With the current results, the calibration error has been effectively eliminated from the microwave measurements of μ in $^{13}CH_3{}^{12}CD_3$ and $^{12}CH_3{}^{13}CD_3$ (8). The Zeeman study has led to the determination of $g_\parallel$ and $g_\perp$, the g factors, respectively, for rotation about the CC bond and for rotation about an axis perpendicular to the CC bond. The anisotropy $(\chi_\parallel - \chi_\perp)$ in the magnetic susceptibility has been calculated. The Stark and Zeeman parameters determined are listed in Table I.

2. Theory

The torsion−rotation Hamiltonian H_{TR} for a sym-

metric rotor in the ground vibronic state has been discussed by many authors (11, 15, 16). In a recent paper (17), H_{TR} has been studied for CH_3SiH_3 in the light of the avoided-crossing experiments (14) and extensive new microwave spectra for torsional levels with $v = 0-4$. Here only the most relevant results will be reviewed and only those terms that enter directly into the analysis of the current data will be retained.

In the internal-axis method (IAM), H_{TR} can be formally written as

$$[1] \quad H_{TR} = H_R^{(0)} + H_T^{(0)} + H_{TR}^{(1)}$$

In zeroth order, the rotational and torsional motions are completely decoupled with $H_R^{(0)}$ and $H_T^{(0)}$, respectively, accounting for these degrees of freedom.

$$[2] \quad H_R^{(0)} = BJ^2 + (A - B)J_z^2$$

$$[3] \quad H_T^{(0)} = Fp^2 + V_3 \tfrac{1}{2}(1 - \cos 3\alpha)$$

The reduced rotational constant $F = A/[\rho(1 - \rho)]$ where $\rho = I_\alpha/(I_\alpha + I_F)$ with I_α and I_F being, respectively, the moments of inertia about the symmetry axis of the CH_3-top and of the CD_3-frame. The first-order Hamiltonian $H_{TR}^{(1)}$ can be expanded in terms of the square of the total angular momentum $\boldsymbol{J}$ (exclusive of nuclear spin), the component J_z of $\boldsymbol{J}$ along the symmetry axis $\hat{z}$, the torsional angular momentum $\boldsymbol{p}$, and the Fourier factor $\frac{1}{2}(1 - \cos 3\alpha)$. If only the terms included in the least squares fit are retained, then

$$[4] \quad H_{TR}^{(0)} = -D_J J^4 - D_{JK} J^2 J_z^2 - D_K J_z^4 - D_{Jm} J^2 p^2 - d_J J^2 J_z p + F_{3J} \tfrac{1}{2}(1 - \cos 3\alpha) J^2$$

The largest term neglected in the hindering potential $V(\alpha)$ is $V_6 \frac{1}{2}(1 - \cos 6\alpha)$. The value of ρ in first order will deviate from that given by the zeroth-order expression. A detailed discussion of the effective parameters resulting from truncating $H_{TR}^{(1)}$ as shown in [4] is given elsewhere (17).

The torsion–rotation energies can be labelled by the quantum numbers (v, J, K, σ, m_J). The symmetry type of the torsional sublevels is A for $\sigma = 0$ and E for $\sigma = \pm 1$. The correspondence between the torsion–rotation symmetry Γ characterizing the irreducible representations of the group G_{18} is given by Hirota (18). m_J is the eigenvalue of the component $\boldsymbol{J}$ along the space-fixed $\hat{Z}$ axis, which is defined by the direction of $\boldsymbol{\epsilon}$. If the nuclear hyperfine energy is taken into account, the magnetic quantum numbers m_H and m_D must be introduced; these are associated, respectively, with the total hydrogen nuclear spin $\boldsymbol{I}_H$ and the total deuterium spin $\boldsymbol{I}_D$. The magnetic quantum number for the total angular momentum is $m_T = (m_J + m_H + m_D)$.

3. Experimental details

The experimental methods and conditions were very similar in many respects to those used for earlier studies of symmetric rotors (2, 19, 20). The basic molecular-beam electric-resonance apparatus has been described elsewhere (21). The sample of CH_3CD_3 was supplied by Merck, Sharp, and Dohme of Canada with a specified isotopic enrichment of 98%. No further purification was necessary. The data were taken with the mass spectrometer tuned to the ion peak with a mass-to-charge ratio of 30. To facilitate the state selection by the electric quadrupole fields, the source was cooled to −50°C, thereby slowing the beam significantly. To concentrate the population in the lower rotational levels, the seeded beam technique was used. A mixture of 4% CH_3CD_3 in argon was expanded through a 40 μm nozzle. The backing pressure was adjusted for each line to give the most intense signal. The optimum values ranged from 1.0 to 1.4 bar (1 bar = 100 kPa); lower pressures were needed for the states of higher J and K to prevent the depopulation of these higher energy states in the expansion.

The studies carried out were limited to relatively low J and K primarily because of the difficulty in focussing a molecule with such a small dipole moment (~0.01 D); only states with a relatively fast linear Stark effect could be deflected adequately. The quadrupolar selecting fields were originally designed (2) to maintain high electric fields and this feature was essential to the present experiment. The electrostatic lenses were carefully cleaned and polished to minimize cold emission and breakdown. The maximum field gradient attainable was ~200 kV/cm; this maximum was used for all the transitions studied.

Relatively high C fields were required both in the Stark–Zeeman studies to maximize the accuracy and in the avoided-crossing experiments to reach the crossing regions. To generate these field strengths with the necessary homogeneity and stability, the Pyrex C field and the stabilization system developed earlier (20) were used. The long-term stability and resettability of the voltage was ≲20 ppm, while the short-term stability was ≲2 ppm. The homogeneity requirements were not as stringent for CH_3CD_3 as for earlier symmetric tops studied such as CF_3H (20), because the Stark effects here were so much smaller. The narrowest line widths were attained using the full 10-cm length of the Pyrex plates. The plate configuration was set for ($\Delta m_T = \pm 1$) transitions for the Stark–Zeeman studies and for ($\Delta m_T = 0$) transitions for the avoided-crossing measurements.

4. The Stark effect

A precision study of the Stark effect in CH_3CD_3 was carried out by conventional molecular-beam electric resonance methods (19, 22, 23). In the infinite barrier limit, the effective dipole moment characterizing

matrix elements diagonal in J and K is given by (23, 24)

$$[5] \quad \mu_Q(J,K) = \mu_0 + \mu_J J(J+1) + \mu_K K^2$$

Here μ_0 is the rotationless dipole moment in the ground vibronic state; μ_J and μ_K are the lowest-order centrifugal distortion constants. For finite V_3, some torsional terms have to be added (23), but these are too small to be significant here. To complete the characterization of the Stark effect to this order in CH_3CD_3, it is necessary to introduce only one more parameter, namely $(\alpha_\parallel - \alpha_\perp)$. In general, it is the effective anisotropy $(\alpha_\parallel - \alpha_\perp)_{\text{eff}}$ that enters (23). However, in the present case, the difference can be neglected because it is very small, being proportional as it is to μ_0/B (23).

To determine the four Stark parameters, ($\Delta J = 0$, $\Delta K = 0$, $\Delta m_J = \pm 1$) spectra were studied for $J_{\pm|K|} = 1_{\pm 1}$, $2_{\pm 1}$, $2_{\pm 2}$, $3_{\pm 1}$, $3_{\pm 2}$, and $3_{\pm 3}$; states with $K = 0$ have only a quadratic Stark effect and so could not be focussed. Except for the $1_{\pm 1}$ spectrum, each spectrum appeared as a structureless feature whose full width at half-maximum ranged from 7 to 20 kHz, being a combination of unresolved hyperfine splitting and the time-of-flight line width of 5.2 kHz. The $1_{\pm 1}$ spectrum consisted of three narrow features; the splittings in the triplet were slightly asymmetric with the central line (11.8 ± 1.0) kHz from the highest component and (12.7 ± 1.0) kHz from the lowest.

The small magnitude of μ_0 complicated the experiment in several ways. First, as indicated in Sect. 3, it was very difficult to focus the beam. To detect a transition, a relatively fast linear Stark effect was required; measurements were therefore restricted to the low values of J and $|K|$ listed above. Further, an optimum change in the Stark effect was required between the A and B fields. As a result, only ($m_J = \mp 1 \rightarrow 0$) transitions could be detected efficiently.

The second difficulty arising from the small value of μ is associated with the asymmetric broadening introduced by the nuclear hyperfine effects into each $J_{\pm|K|}$ spectrum (19, 23). In the $1_{\pm 1}$ case, the effects are large enough to produce the asymmetric splitting indicated above. For the $3_{\pm 2}$ case, the quadrupole and spin–spin interactions vanish and the broadening is symmetric. If μ in CH_3CD_3 were ~1 D, then for a general $J_{\pm|K|}$ the shift $\delta\nu_{\text{hyp}}$ of the center of the spectrum away from the hyperfine-free value could be made negligible simply by raising the transition frequency to several hundred MHz, as was done in CH_3SiH_3 (23). Because μ is only ~0.010 D, an alternative method was required. Measurements were made at several different fields and a different intercept $\delta\nu_{\text{hyp}}$ was introduced as a fitting parameter for each $J_{\pm|K|}$, except $3_{\pm 2}$ for which $\delta\nu_{\text{hyp}} \equiv 0$ and $3_{\pm 1}$ for which $\delta\nu_{\text{hyp}} \ll$ the experimental error. The results are summarized in Table 2. The splitting of the $1_{\pm 1}$ spectrum was found to be independent of ϵ; this fact and the small magnitudes obtained for $\delta\nu_{\text{hyp}}$ confirm the validity of this approach.

The third difficulty arises from the fact that the second-order Stark effect is very small. As a result, the $2_{\pm 1}$ and $3_{\pm 2}$ spectra, having identical linear Stark coefficients, could not be resolved even at the highest ϵ fields available. To overcome this problem, the data for $2_{\pm 1}$ and $3_{\pm 2}$ were taken with an external magnetic field $\boldsymbol{B}$ of 0.3 T applied parallel to $\boldsymbol{\epsilon}$. As discussed in Sect. 5, the spectrum for each $J_{\pm|K|}$ splits into two Zeeman components. Because the effective g factor $g(J,K)$ is different for $2_{\pm 1}$ and $3_{\pm 2}$, it is then possible to resolve the two spectra. The identification of the lines was straightforward once the Zeeman measurements on the other $J_{\pm|K|}$ transitions were completed. For each $J_{\pm|K|}$, the frequency for the ($B \rightarrow 0$) limit can be taken as he average of the frequencies of the corresponding Zeeman components. In general, this will introduce an error $\delta\nu_{\text{sus}}$ proportional to B^2 and to the anisotropy $(\chi_\parallel - \chi_\perp)$ in the magnetic susceptibility. For $3_{\pm 2}$, $\delta\nu_{\text{sus}} \equiv 0$ because the contribution of $(\chi_\parallel - \chi_\perp)$ to the energy vanishes. For $2_{\pm 1}$, with $B = 0.3$ T and the value of $(\chi_\parallel - \chi_\perp)$ obtained in Sect. 5, this contribution reduces the magnitude of the frequency of each Zeeman component (and hence of the average) by 0.29 kHz. However, no correction has to be added specifically for this effect. Because $\boldsymbol{B}$ was the same for all measurements on the $2_{\pm 1}$ spectrum, $\delta\nu_{\text{sus}}$ is constant and so will be equivalent to an additional hyperfine shift: $\delta\nu_{\text{sus}}$ is simply absorbed into $\delta\nu_{\text{hyp}}$. This method of determining the Stark frequencies for $2_{\pm 1}$ and $3_{\pm 2}$ makes use of the fact that the hyperfine shift is also independent of $\boldsymbol{B}$. This point was confirmed by a study of the $1_{\pm 1}$ spectrum as a function of $\boldsymbol{B}$.

For any $J_{\pm|K|}$, small systematic errors can be introduced if $\boldsymbol{J}$ is not decoupled from the nuclear spins for all the data (19). To avoid such "decoupling shifts," the earlier data for $1_{\pm 1}$, $2_{\pm 2}$, and $3_{\pm 3}$ were taken in a small magnetic field of ~1 mT. The study mentioned above the $1_{\pm 1}$ spectrum as a function of B showed that these shifts are negligible and the later data on these spectra as well as the measurements for $3_{\pm 1}$ were taken in the earth's field.

The electric fields were calibrated using the OCS spectrum in the ground vibronic state. Two transitions were used, either ($J = 1$, $m_J = \pm 1 \rightarrow 0$) or ($J = 2$, $m_J = \pm 2 \rightarrow \pm 1$). The OCS Stark parameters taken were $\mu = 0.71519(3)$ D (25) and $(\alpha_\parallel - \alpha_\perp)_{\text{eff}} = 4.67(8)$ Å^3 (26).

The final Stark measurements are listed in Table 2. The least-squares analysis in terms of the four Stark parameters and the various hyperfine shifts yielded a good fit, as can be seen from the differences listed in Table 2 between the observed and calculated frequencies. The four Stark parameters are given in

TABLE 2. Stark measurements[a,b]

	$1_{\pm1}$		$2_{\pm1}$		$2_{\pm2}$		$3_{\pm1}$		$3_{\pm2}$		$3_{\pm3}$	
ϵ(V/cm)	ν	δ	ν	δ	ν	δ	ν	δ	ν	δ	ν	δ
567.7622	1 551.7(4)	0.3										
852.2298	2 329.5(5)	−0.1	777.0(4)	0.0					776.6(3)	−0.1		
852.2334					1551.6(5)	0.2						
1 137.0731											1 551.5(12)	0.0
3 316.566			3 023.9(8)	0.5					3 022.7(4)	0.0		
3 316.574	9 065.7(5)	0.1			6 040.7(10)	−0.2					4 528.0(14)	0.0
6 633.441			6 047.3(4)	0.1					6 045.9(4)	0.1		
6 633.473	18 131.2(5)	0.8			12 081.9(14)	−0.9						
11 385.996					20 737.9(4)	0.0						
11 386.518	31 115.9(7)	−0.6										
11 494.758							5242.7(60)	−0.5				
13 266.972			12 094.7(7)	−0.8					12 091.6(5)	0.1		
13 267.228	36 253.8(7)	0.0										
13 267.335					24 163.5(14)	0.0						

[a]All frequencies are in kHz for $m_J = \mp 1 \rightarrow 0$. The number listed in parentheses following each ν is the experimental error. δ is the difference between the measurement and the best-fit value.

[b]The hyperfine shifts $\delta\nu_{hyp}$ deduced from the fit were, in kHz: −0.2(2) for $1_{\pm1}$; 0.0(2) for $2_{\pm1}$; −1.4(3) for $2_{\pm2}$; −1.6(5) for $3_{\pm3}$. For $3_{\pm2}$, $\delta\nu_{hyp} \equiv 0$ on theoretical grounds.

Table 1. It was possible to determine $(\alpha_\parallel - \alpha_\perp)$ to the accuracy indicated because $(\alpha_\parallel - \alpha_\perp)$ contributed most of the quadratic Stark effect. This contribution was very important in another regard. Although it was expected on the basis of the focussing arguments given above that the $(m_J = \mp 1 \rightarrow 0)$ component dominated each $J_{\pm|K|}$ spectrum, some independent check of this m_J identification was required. The quadratic contribution from $(\alpha_\parallel - \alpha_\perp)$ was large enough that the quality of fit was able to provide this check.

It had been determined earlier from microwave experiments (7) that $\mu = 0.01078(9)$ D. If centrifugal distortion is taken into account, this value corresponds to $\mu_0 + \mu_K$ (23); however, the value of μ_K is small compared with the experimental uncertainty of ~1%. The microwave and molecular beam determinations are in good agreement.

The microwave value for $^{12}CH_3{}^{12}CD_3$ was subsequently used to calibrate the electric field in a measurement of μ in two ^{13}C isotopic modifications (8). The accuracy of these two determinations can now be improved by using $(\mu_0 + \mu_K)$ from Table 1 here. The results are that $\mu = 0.01075(3)$ D for $^{13}CH_3{}^{12}CD_3$ and 0.01102(5) D for $^{12}CH_3{}^{13}CD_3$. See Table II of ref. 8.

The optical anisotropy $(\alpha_\parallel - \alpha_\perp)_{opt}$ has been measured in CH_3CH_3 by light scattering techniques (27, 28). If the data of Bogaard *et al.* (27) at $\lambda = 4880$, 5145, and 6328 Å are extrapolated to zero frequency using the linear dependence on ν^2 suggested (29) by data on other molecules, then a $(\nu = 0)$ value of 0.68 Å^3 is obtained, which does not differ significantly from the current determination. Since the extrapolated optical value should differ from the static Stark effect result by the vibrational contribution, it can be concluded that this vibrational contribution is small.

5. The Zeeman effect

The method of determining rotational g factors by molecular-beam electric-resonance spectroscopy has been described in detail elsewhere (19, 23). When $\boldsymbol{B}$ is applied parallel $\boldsymbol{\epsilon}$, each $(\Delta J = 0, \Delta m_J = \pm 1)$ line splits into two; the separation is $2\mu_N B|g(J,K)|$ where

$$[6] \quad g(J,K) = g_\perp + (g_\parallel - g_\perp)K^2/J(J+1)$$

μ_N is the nuclear magneton. Contributions from the nuclear shielding and from internal rotation can be neglected here.

Detailed Zeeman measurements were made for $B = 0.4$ and 0.8 T; three different spectra were studied. It was found that, in nuclear magnetons, $|g(1,1)| = 0.08384(6)$, $|g(2,2)| = 0.11083(16)$, and $|g(3,2)| = 0.05700(6)$. From these values, the magnitudes of $g_\parallel$ and $g_\perp$ were obtained; it was also shown that the two g factors have the same sign. The results are given in Table 1. Measurements of lower accuracy were made of $|g(2,1)|$; these acted as further confirmation of the identification of the $3_{\pm 2}$ and $2_{\pm 1}$ spectra.

A serious attempt was made to determine experimentally the absolute sign of the g factors by studying the Zeeman effect on the EA avoided crossing $(J = 1, K = \pm 1, m_J = \mp 1, \sigma = \mp 1) \leftrightarrow (1, \mp 1, 0, 0)$. This method of sign determination has been discussed in detail previously (2). Unfortunately, no definitive conclusion could be reached. Because $\Delta m_J \neq 0$ in the anticrossings used for this purpose, the resulting spectra can receive frequency contributions from the major hyperfine interactions. Unlike previous studies (2, 13, 20, 23), the CH_3CD_3 spectra showed complicated hyerpfine patterns of clearly resolved lines. Without a detailed understanding of the hyperfine problem, the sign of the g factors could not be established.

No attempt was made to measure the anisotropy $(\chi_\parallel - \chi_\perp)$ in the susceptibility. However, a value can be calculated from the g factors and the molecular quadrupole moment $\theta_\parallel$ using [14] of ref. 19. With $\theta_\parallel = -(2.67 \pm 0.33) \times 10^{-40}$ cm^2 (30), it was found that $(\chi_\parallel - \chi_\perp) = -90.2 \times 10^{-30}$ J/T^2 if the g factors are positive and $+113.7 \times 10^{-30}$ J/T^2 if the g factors are negative. From a survey of g factors and susceptibility anisotropies for related molecules such as $CH_3—C{\equiv}C—H$ (31), it is clear that, for CH_3CD_3, $g_\parallel$ must be positive and $(\chi_\parallel - \chi_\perp)$ must be negative. The results are summarized in Table 1. The error in $(\chi_\parallel - \chi_\perp)$ of 1.7% is entirely due to the uncertainty in $\theta_\parallel$. However, the value of $(\chi_\parallel - \chi_\perp)$ is very insensitive to $\theta_\parallel$; if $\theta_\parallel$ were to change by 50%, $(\chi_\parallel - \chi_\perp)$ would change by only 6.7%.

6. The avoided-crossing measurements

The energy levels involved in the barrier anticrossings for $J = 1$ are illustrated in Fig. 1. Each level is labelled by the high-field quantum numbers that apply when $\epsilon \ll \epsilon_c$. Each of the anticrossings are between upper level $(\alpha) \equiv (J, K_\alpha = \pm 1, \sigma_\alpha, \Gamma_\alpha)$ and lower level $(\beta) \equiv (J, K_\beta = \mp 1, \sigma_\beta, \Gamma_\beta)$. When the magnetic quantum numbers are taken into account, each "level" in Fig. 1 is really a family of levels whose energies far from ϵ_c differ only in the hyperfine terms. Thus the possibility must be considered that each anticrossing can involve interactions among many states (2, 14). However, when a significant magnetic field $\boldsymbol{B}$ is applied, the anticrossings in which all magnetic quantum numbers are conserved are well separated in crossing field from the other possibilities. It is these particular anticrossings that are of interest here. In this case, each single (α) level interacts with one and only one (β) level; the anticrossing can be analysed as a series of two-level problems.

These $(\Delta m_J = 0)$ anticrossings have the advantage

TABLE 3. Energy splittings Δ_0 in MHz and ratios of splittings from anti-crossing experiments[a] in CH_3CD_3

Label[b]	Observed	Observed − Calculated
$\nu_{EA}(J = 1)$	26.32636(120)	−0.0002
$\nu_{EE}(J = 1)$	17.21660(77)	[c]
$\nu_{EA}(J = 2)$	26.32046(90)	0.00015
$\nu_{EE}(J = 2)$	17.21544(62)	−0.00004
$\nu_{EA}(J = 1)/\nu_{EE}(J = 1)$	1.529125(10)	0.000000
$\nu_{EA}(J = 2)/\nu_{EE}(J = 2)$	1.528874(14)	−0.000001
$\nu_{EA}(J = 1)/\nu_{EE}(J = 2)$	1.529248(68)	0.000010

[a]All measurements are in the ground torsional state.

[b]$\nu_{EA}(J) \equiv \Delta_0$ for $(J, K = \pm 1, \sigma = \mp 1, \Gamma = E_3) \leftrightarrow (J, \mp 1, 0, E_1)$; $\nu_{EE}(J) \equiv \Delta_0$ for $(J, K = \pm 1, \sigma = \mp 1, \Gamma = E_3) \leftrightarrow (J, \mp 1, \mp 1, E_2)$.

[c]This was not included in the fit because this same measurement has been used in a ratio.

that the zero-field separation Δ_0 between the interacting levels depends only on the torsional splittings. Further, ϵ_c is independent of the Zeeman effect and the second-order Stark effect. These two statements apply because the only possible differences between the α and β quantum numbers are in σ and in the *sign* of K. While both statements fail to take into account certain σ-dependent terms, these are negligible here. These barrier anticrossings are therefore very well suited to precision studies of internal rotation.

For the energy level system shown in Fig. 1, two different anticrossings were observed. For ϵ_c = 3148.85(10) V/cm, $(\Gamma_\alpha = E_3) \leftrightarrow (\Gamma_\beta = E_2)$. Since $(\sigma_\alpha = \mp 1) \leftrightarrow (\sigma_\beta = \mp 1)$, both levels are of E torsional symmetry; this is called an EE anticrossing with its Δ_0 denoted ν_{EE}. For ϵ_c = 4814.98(9) V/cm, $(\Gamma_\alpha = E_3) \leftrightarrow (\Gamma_\beta = E_1)$. Here $(\sigma_\alpha = \mp 1) \leftrightarrow (\sigma_\beta = 0)$; the torsional symmetry changes from E to A. This is called an EA anticrossing with its Δ_0 denoted ν_{EA}. A serious attempt was made to observe the third anticrossing with $(\Gamma_\alpha = E_2) \leftrightarrow (\Gamma_\beta = E_1)$, but this was unsuccessful. A similar study was made for the corresponding anticrossing system with $J = 2$ and $m_J = \pm 2$; similar results were obtained. For higher values of J, the quadrupole fields could not provide adequate focussing. All observations were made in the ground torsional state.

Precision crossing field measurements were made for the EA and EE barrier anticrossings for $J = 1$ and $J = 2$ for $(m_J = \pm 1 \rightarrow \pm 1)$ and $(m_J = \pm 2 \rightarrow \pm 2)$, respectively. In each case, the value of Δ_0 was determined using the dipole constants given in Table 1. The results are given in Table 3. The accuracy in Δ_0 is limited by the calibration of the electric field strength and the uncertainty in μ_0. Relative measurements were made for three pairs of anticrossings using the splitting method described in Sect. II of ref. 20. In each case, the ratio of the two Δ_0 was determined and the result given in Table 3. In such a ratio measurement, the uncertainty

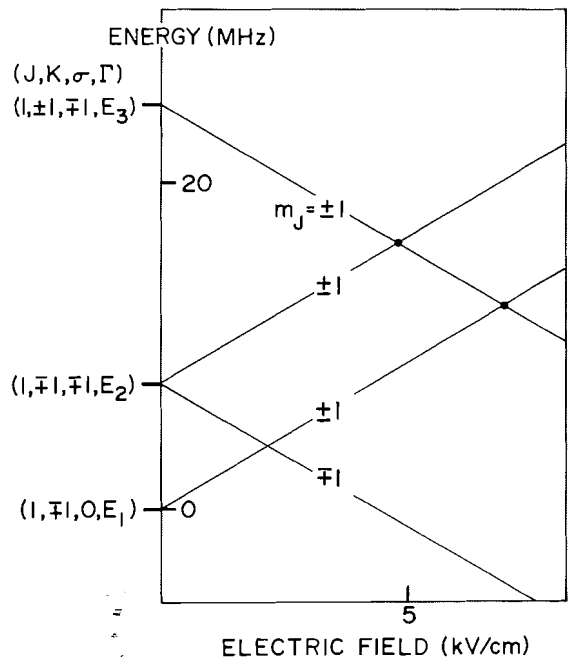

FIG 1. Schematic plot against the electric field of the energy levels with $(J, K) = (1, \pm 1)$ in CH_3CD_3 that are involved in the anticrossings studied. The two heavy dots indicate the avoided crossings which have been detected. For each dot, the upper signs go with upper and the lower signs with lower.

in μ_0 cancels and an independent field calibration is unnecessary. The accuracy in the ratio is limited by the short-term stability (2 ppm) of the electric field and the error in measuring the line centres in the avoided-crossing spectra. The full width at half-maximum for a line far from ϵ_c was typically 5 kHz and the frequency errors were about a factor of 10 smaller. In many cases, the ratio measurements have a higher percent accuracy than the absolute determinations of Δ_0. The results in

TABLE 4. Observed minimum separation ν_{min} in the barrier anticrossings in CH_3CD_3

J	Label	ν_{min} (kHz)
1	EA^a	8.49(29)
2	EA^a	13.48(38)
1	EE^b	36.22(16)
2	EE^b	51.98(29)

[a] $(K = \pm 1, \sigma = \mp 1, \Gamma = E_3) \leftrightarrow (\mp 1, 0, E_1)$.
[b] $(K = \pm 1, \sigma = \mp 1, \Gamma = E_3) \leftrightarrow (\mp 1, \mp 1, E_2)$.

Table 3 are analysed in Sect. 7.

The origin of the matrix element η that mixes the two interacting levels is of considerable interest. As argued earlier (13, 14), η must arise from the nuclear hyperfine interactions. It seems to be a general property of the mixing that the second EE anticrossing corresponding to $(\Gamma_\alpha = E_2) \leftrightarrow (\Gamma_\beta = E_1)$ in Fig. 1 cannot be detected. This negative result has now been obtained for CH_3CD_3, CH_3SiH_3 (14), and CH_3SiF_3 (13). Preliminary results of the ongoing hyperfine analysis show that the missing EE crossing can only be driven by an interaction which changes the symmetry of both the hydrogen spin function and the deuterium spin function. The deuterium quadrupole interaction does not involve the hydrogen spin operators and so cannot provide the necessary mixing. In spite of the growing body of evidence that η for the second EE crossing is either identically zero or very small, a definitive conclusion cannot be reached until a detailed explanation is developed.

Further insight into the hyperfine problem can be obtained by measuring η for the allowed anticrossings. In the earlier studies where η arose from hyperfine effects, $|\eta|$ was so small that a direct measurement from the curvature of the energy levels near ϵ_c could not be made. However, in CH_3CD_3, the minimum separation ν_{min} between the interacting levels was larger than the line width and measurements could be made at frequencies $\sim\nu_{min}$ for each of the four anticrossings studied. The resulting values of ν_{min} are listed in Table 4. Because each anticrossing can be treated as a two-level problem, $|\eta| = \nu_{min}/2$ (2).

Preliminary calculations of the hyperfine matrix elements off-diagonal in Γ allow several conclusions to be drawn about η from these measurements. First, the J dependence of η is consistent with the assumption that the mixing is provided either by a nuclear spin–spin interaction or by the nuclear quadrupole coupling terms. The dipolar coupling constants can be calculated from the nuclear g factors and the molecular structure. The deuterium quadrupole coupling constant eqQ = (167 ± 18) kHz (32). From these constants and the values of $|\eta|$ in Table 4, it appears that the hydrogen–hydrogen dipolar interaction drives the EA anticrossings, and the deuterium quadrupole interaction provides the mixing for the EE cases. A detailed analysis of the nuclear hyperfine interactions in a molecule of G_{18} symmetry is currently underway.

TABLE 5. Rotational frequencies of CH_3CD_3 used in the internal rotation fit[a]

v	$J' \leftarrow J''$	$K' = K''$	Frequency[b] (MHz)	Ref.
0	2 ← 1	±1	65 896.923(50)	7
0	3 ← 2	±1	98 844.21(10)	8
0	3 ← 2	±2	98 843.31(15)	8
1	2 ← 1	±1	- 65 675.536(50)[c]	7

[a] Because there are no degrees of freedom in this portion of the least squares analysis, the fit to these frequencies is exact. See Sect. 7.
[b] The A and E satellites were not resolved.
[c] The identification has been confirmed by an analysis of the torsional spectrum. See footnote 1 to the text.

7. Internal rotation: analysis and discussion

In addition to the avoided-crossing data presented in Sect. 6, there are available pure rotational frequencies measured by microwave absorption (7, 8). These are summarized in Table 5 here. In each case the σ splitting was not resolved. The assignment in ref. 7 of the (v = 1) line has been confirmed by recent studies[1] of the torsional spectrum of CH_3CD_3.

A detailed least squares analysis of the data in Tables 3 and 5 was carried out using [2]–[4] and methods described previously (13, 14, 17). A good fit was obtained. The constants determined are listed in Table 1. There are only two degrees of freedom in the analysis; there are 10 pieces of data and eight independent parameters: B, D_J, D_{JK}, ρ, F_{3J}, D_{Jm}, d_J, and the reduced barrier height $s = 4V_3/9F$. D_K was fixed at the force-field value (33). This step should not introduce any significant errors; the same calculation provides values of D_J (19.3 kHz) and D_{JK} (50.9 kHz), which are in excellent agreement with the experimental results.

In order to be in a position to evaluate the effects of fixing various constants at zero, it is important to trace the paths connecting the determined parameters to the experimental data. For a given J, the ratio ν_{EA}/ν_{EE} determines ρ, as can be seen from [21] of ref. 17; $[\nu_{EA}^2 + \nu_{EE}^2 - \nu_{EA}\nu_{EE}]^{1/2}$ determines s (and its error) through the coefficient L in [24a] of ref. 17. The J dependence of ν_{EA} and that of ν_{EE} fix d_J through coefficient B_1 in [22b] of ref. 17 and provide a linear combination of F_{3J} and D_{Jm} through coefficient S in [24b] of ref. 17. The four microwave frequencies determine D_J, D_{JK}, and two linear combinations of B, F_{3J}, D_{Jm}, and d_J, as can be seen from [14] and [15] of ref. 17. With the constraints described above from the beam data, it

TABLE 6. Comparison of the barrier heights V_3 for different isotopic forms of ethane[a]

Isotopic form	n_D	V_3 (cm^{-1})	V_3' (cm^{-1})[b]
CH_3CH_3	0		1 013.29(24)
CH_3CH_2D	1	1 010.24(14)[c]	[f]
CH_3CHD_2	2	1 006.70(98)[d]	1 007.21(13)
CH_3CD_3	3	1 004.13(21)[e]	[f]
CH_2DCD_3	4	1 001.00(385)[c]	1 001.08(32)

[a]All analyses assume $V_6 \equiv 0$.
[b]This is calculated from linear dependence on n_D given in [7].
[c]Reference 10.
[d]Reference 9.
[e]Present work.
[f]This value was used to define the straight line; hence $V_3' \equiv V_3$ in this case.

is clear that the four microwave frequencies can be fit exactly; both of the degrees of freedom lie in the anticrossing measurements. For the beam data, as can be seen from Table 3, the differences between the observed and calculated values are small, but must be interpreted in the light of the small numbers of degrees of freedom. Each of the parameters is contaminated to some extent with contributions from the many constants fixed at zero. Further details are given in ref. 17.

The current results for D_{JK} and D_J are identical to those in ref. 8 since the same relevant data were used. The present value of B cannot be compared directly with that in ref. 8 because the present determination has had the internal-rotation contributions of F_{3J}, D_{Jm}, and d_J removed. Ultimately it would be of interest to determine the structure from a set of such rotational constants.

The value of V_3 is calculated from s by using $F = A/[\rho(1-\rho)]$. As a result, a value of A is required. The best direct experimental value is 53 531(63) MHz obtained by Heise and Cole (34) by reanalysing the Raman data of Shaw and Welsh (35). However, with the recent microwave work on the asymmetrically substituted deuterated ethanes (10) in which accurate A constants were determined, the resulting calculated value of A for CH_3CD_3 should be more accurate. This value of A is 53 499(11) MHz as evaluated from the value of the moment of inertia about the symmetry axis: I_a = 9.4465(20) amu Å^2. This in turn was extracted from the value of I^a_{zz} given in Table IX of ref. 10 and the correction ΔI^a_{vib} given in Table II of ref. 36. The structure value of A is in very good agreement with the experimental value (34). Within the framework of the current model (17), the errors in s and ρ are so small that the error in V_3 is dominated by that in A. If an improved value of A becomes available, the corresponding value of V_3 can be obtained from the present determinations of s and ρ. For any reasonable value of A, the values of the other parameters do not change significantly.

The best previous determinations of V_3 in the ethanes were those by microwave methods for the asymmetrically substituted deuterated modifications (9, 10). The resulting values are compared in Table 6 with the current measurement. In each case, the model assumed sets $V_6 = 0$. For the asymmetric tops, the normal quartic centrifugal distortion constants were taken into account, but no torsion–distortion constants (e.g., F_{3J}) were included. The accuracy of the present measurement is comparable to that for the most favorable asymmetric species, CH_3CH_2D.

As was pointed out by Hirota *et al.* (10), V_3 appears to be a linear function of n_D, the number of deuterons, but the accuracy of the CD_3CH_2D measurement did not permit a sufficiently stringent test of this hypothesis. With the addition of the present result, such a test is now possible. Using the best values in Table 6, namely those for n_D = 1 and 3, the equation of this straight line is, in cm^{-1},

$$[7] \quad V_3' = 1013.29(24) - 3.05(13)n_D$$

Here the intercept 1013.29(24) cm^{-1} is the predicted barrier height for C_2H_6 and −3.05(13) is the change per deuteron of the barrier height in cm^{-1}. Table 6 also lists the empirical values from [7] for n_D = 2 and n_D = 4. These values differ from the experimental numbers by less than the uncertainties in the latter; the linear relationship fits very well. Overall, the consistency between the beam and microwave measurements is excellent. The slope in [7] can be compared with the value of −6.0 cm^{-1} per deuteron, which can be deduced from the results in ref. 37 from the difference between C_2H_6 and C_2D_6.

The largest model error in these values of V_3 is expected to arise from fixing V_6 at zero. From computer experiments, it has been found that high correlations exist among V_3, V_6, and several torsional distortion constants for a data set consisting of torsional splittings for $v = 0$ and even extensive microwave measurements for many different v. To help break the correlations, a study[1] is currently being completed of the far infrared torsional spectrum of CH_3CD_3. The evaluation of V_6 is complicated by the redundancy (16, 17, 38) connecting V_6 with higher-order torsional terms. At the moment, the best estimate for the effective value of V_6 is (7.0 ± 3.5) cm^{-1}, as determined for CH_3CHD_2 (10). If this value (with its error) is adopted for CH_3CD_3 and the current data reanalysed, then V_3 = (998.6 ± 3.0) cm^{-1}; the error reflects only the stated uncertainty in V_6 and does not cover any possible isotopic change in V_6. The other parameters in Table 1 do not change significantly.

The measurement of ρ in a molecule such as CH_3CD_3 offers an unusual opportunity to study the effects of deuteration on the structure. To the order considered

here, $\rho = I_\alpha/I_a$. If the perpendicular distance X_H of the hydrogen atom from the symmetry axis equals the corresponding distance X_D of a deuterium atom, then $\rho = M_H/[M_H + M_D]$, where M_H and M_D are the hydrogen and deuterium masses, respectively. On the other hand, if $\lambda \equiv (X_H - X_D) \neq 0$, then to first order in λ/X_H,

$$[8] \quad \rho = \frac{M_H}{[M_H + M_D]}\left\{1 + \frac{2M_D}{[M_H + M_D]}\frac{\lambda}{X_H}\right\}$$

λ/X_H can easily be related to the CH bond length r_{CH}, the acute angle θ_H between the CH bond and the symmetry axis, and the corresponding quantities r_{CD} and θ_D for the CD bond.

$$[9] \quad \lambda/X_H = [r_{CH} - r_{CD}]/r_{CH} + (\theta_H - \theta_D)/\tan\theta_H$$

Thus the deviation of ρ from $M_H/[M_H + M_D]$ is a direct measure of the structural changes that occur upon deuteration. This measure is unusual in that it arises from a comparison of the deuterated unit with an equivalent protonated unit in the same molecule, rather than from a comparison between different molecules. Unfortunately, there are higher-order effects (17) which can make $(\rho - I_\alpha/I_a)$ non-zero and obscure the structural information in [8].

With the information currently available, there are two alternative methods of applying [8]. First, the magnitude of the higher-order torsional effects on ρ can be estimated. From the structure given in Table VIII of ref. 10, $\lambda/X_H = 0.83(20) \times 10^{-3}$ and $(I_\alpha/I_a) = 0.333872(87)$, so that $(\rho - I_\alpha/I_a) = (1.1 \pm 0.9) \times 10^{-4}$. This indicates that the errors of this type limit the accuracy of values of I_α determined from ρ to ~300 ppm. To our knowledge, this is the first independent measurement of these higher-order effects in internal rotation.

The moment of inertia I_α of the CH_3 top can be calculated from ρI_a now by assigning an error of 1×10^{-4} to ρ. With the ground state value of $I_a = 9.4465(20)$ amu Å^2 deduced above from ref. 10 and ref. 36, $I_\alpha = 3.1549(12)$ amu Å^2. This is very close to the values obtained earlier: for CH_3SiH_3, $I_\alpha = 3.165(5)$ amu Å^2 (14); for CH_3SiF_3, $I_\alpha = 3.170(2)$ amu Å^2 (13).

In the alternative method of applying [8], λ/X_H can be calculated from ρ in Table 1 by assuming that such higher-order effects are negligible. If this is done, then $\lambda/X_H = 1.069(6) \times 10^{-3}$, in good agreement with the structure value of $0.83(20) \times 10^{-3}$ given above. The magnitude of this ratio is dominated by the bond-length term in [9]. It is clear that if it can be shown on independent grounds that $|\rho - I_\alpha/I_a| \ll 10^{-4}$, then the current measurement of ρ can be used to obtain valuable new insight into the structure.

NOTE ADDED IN PROOF: It is of interest to compare the current values of $(\chi_\parallel - \chi_\perp)$ and $(\alpha_\parallel - \alpha_\perp)$ with those that have appeared very recently in a paper by W. Hüttner, H. Häussler, and W. Majer, Chem. Phys. Lett. **109**, 359 (1984). This reference gives $(\chi_\parallel - \chi_\perp) = -97.1(6.8) \times 10^{-30}$ J/T^2 from the Zeeman effect on the $(J = 1 \leftarrow 0)$ microwave transition, in good agreement with the value given here in Table 1. From Hüttner *et al.*, the value of $(\alpha_\parallel - \alpha_\perp)$ extrapolated to zero frequency is 0.632(66) Å^3. This result was obtained from the Cotton–Mouton effect and is based on these authors' value for $(\chi_\parallel - \chi_\perp)$. If the current determination of $(\chi_\parallel - \chi_\perp)$ is used, then the above-mentioned extrapolation yields $(\alpha_\parallel - \alpha_\perp) = 0.680(71)$ Å^3. In either case, the agreement with the value given here in Table 1 is good, but the agreement for the latter is better. The current measurement of the static anisotropy in the polarizability lends considerable support to the arguments presented by Hüttner *et al.* that the higher values for $\Delta\alpha$ in their Table 1 are to be considered more reliable.

Acknowledgements

The authors are grateful to Dr. H. Jagannath, Dr. M. Wong, and Dr. J. K. G. Watson for many fruitful discussions, and to Dr. A. Dymanus for his stimulating interest in the problem. One of us (I.O.) wishes to express his appreciation to the Natural Sciences and Engineering Research Council of Canada for its support. Both authors would also like to thank the National Research Council of Canada for its hospitality while part of the manuscript was being completed and the North Atlantic Treaty Organization Research Grant Program for its support through Travel Grant 1454.

1. W. L. MEERTS and I. OZIER. Phys. Rev. Lett. **41**, 1109 (1978).
2. I. OZIER and W. L. MEERTS. Can. J. Phys. **59**, 150 (1981).
3. S. WEISS and G. E. LEROI. J. Chem. Phys. **48**, 962 (1968).
4. J. SUSSKIND, D. REUTER, D. E. JENNINGS, S. J. DAUNT, W. E. BLASS, and G. W. HALSEY. J. Chem. Phys. **77**, 2728 (1982).
5. L. HENRY, A. VALENTIN, V. M. DEVI, P. P. DAS, K. N. RAO, W. J. LAFFERTY, and J. T. HOUGEN. J. Mol. Spectrosc. **100**, 260 (1983).
6. S. J. DAUNT, A. T. ATAKAN, W. E. BLASS, G. W. HALSEY, D. E. JENNINGS, D. C. REUTER, J. SUSSKIND, and J. W. BRAULT. Astrophys. J. **280**, 921 (1984).
7. E. HIROTA and C. MATSUMARA. J. Chem. Phys. **55**, 981 (1971).
8. E. HIROTA, K. MATSUMURA, M. IMACHI, M. FUJIO, Y. TSUNO, and C. MATSUMURA. J. Chem. Phys. **66**, 2660 (1977).
9. E. HIROTA, S. SAITO, and Y. ENDO. J. Chem. Phys. **71**, 1183 (1979).
10. E. HIROTA, Y. ENDO, S. SAITO, and J. L. DUNCAN. J.

Mol. Spectrosc. **84**, 285 (1981).
11. C. C. LIN and J. D. SWALEN. Rev. Mod. Phys. **31**, 841 (1959).
12. W. GORDY and R. L. COOK. Microwave molecular spectra. Interscience, New York, NY. 1970.
13. W. L. MEERTS and I. OZIER. Chem. Phys. **71**, 401 (1982).
14. W. L. MEERTS and I. OZIER. J. Mol. Spectrosc. **94**, 38 (1982).
15. B. KIRTMAN. J. Chem. Phys. **37**, 2516 (1962).
16. R. M. LEES and J. G. BAKER. J. Chem. Phys. **48**, 5299 (1968).
17. M. WONG, I. OZIER, and W. L. MEERTS. J. Mol. Spectrosc. **102**, 89 (1983).
18. E. HIROTA. J. Mol. Spectrosc. **43**, 36 (1972).
19. W. L. MEERTS, I. OZIER, and A. DYMANUS. Can. J. Phys. **57**, 1163 (1979).
20. W. L. MEERTS and I. OZIER. J. Chem. Phys. **75**, 596 (1981).
21. F. H. DE LEEUW and A. DYMANUS. J. Mol. Spectrosc. **48**, 427 (1973); F. H. DE LEEUW. Ph.D. thesis, Katholieke Universiteit, Nijmegen, The Netherlands. 1971.
22. T. C. ENGLISH and J. C. ZORN. *In* Methods of experimental physics. Vol. 3. *Edited by* D. Williams. Academic Press, New York, NY. 1973.
23. I. OZIER and W. L. MEERTS. J. Mol. Spectrosc. **93**, 164 (1982).
24. J. K. G. WATSON, M. TAKAMI, and T. OKA. J. Chem. Phys. **70**, 5376 (1979).
25. J. M. L. J. REINARTZ and A. DYMANUS. Chem. Phys. Lett. **24**, 346 (1974).
26. L. H. SCHARPEN, J. S. MUENTER, and V. W. LAURIE. J. Chem. Phys. **53**, 2513 (1970).
27. M. P. BOGAARD, A. D. BUCKINGHAM, R. K. PIERENS, and A. H. WHITE. J. Chem. Soc. Faraday Trans. I, **74**, 3008 (1978).
28. F. BAAS and K. D. VAN DEN HOUT. Physica, **95A**, 597 (1979).
29. G. R. ALMS, A. K. BURNHAM, and W. H. FLYGARE. J. Chem. Phys. **63**, 3321 (1975).
30. A. D. BUCKINGHAM, R. L. DISCH, and D. A. DUNMUR. J. Am. Chem. Soc. **90**, 3104 (1968).
31. W. H. FLYGARE and R. C. BENSON. Mol. Phys. **20**, 225 (1971).
32. F. S. MILLETT and B. P. DAILEY. J. Chem. Phys. **56**, 3249 (1972).
33. I. NAKAGAWA and T. SHIMANOUCHI. J. Mol. Spectrosc. **39**, 255 (1971).
34. H. M. HEISE and A. R. H. COLE. J. Mol. Spectrosc. **80**, 320 (1980).
35. D. E. SHAW and H. L. WELSH. Can. J. Phys. **45**, 3823 (1967).
36. J. L. DUNCAN, D. C. MCKEAN, and A. J. BRUCE. J. Mol. Spectrosc. **74**, 361 (1979).
37. B. KIRTMAN, W. E. PALKE, and C. S. EWIG. J. Chem. Phys. **64**, 1883 (1976).
38. R. M. LEES. J. Chem. Phys. **59**, 2690 (1973).